



International Conference on Concentrating Solar Power and Chemical Energy Systems,
SolarPACES 2014

Mg-Zn-Al eutectic alloys as phase change material for latent heat thermal energy storage

E. Risueño^a, A. Faik^{a,*}, J. Rodríguez-Aseguinolaza^a, P. Blanco-Rodríguez^a, A. Gil^a,
M. Tello^b and B. D'Aguzzo^a

^a CIC energigune, Albert Einstein 48, 01510 Miñano (Álava), Spain

^bDpto. Física de la Materia Condensada, Facultad de Ciencia y Tecnología, Universidad del País Vasco, Apdo. 644, 48080 Bilbao, Spain

Abstract

The aim of this study is to investigate high thermal conductive materials such as metallic alloys for latent heat energy storage in CSP applications. For this purposes, two ternary eutectic alloys, $Mg_{70}Zn_{24.9}Al_{5.1}$ and $Zn_{85.8}Al_{8.2}Mg_6$, have been investigated. The structural and thermophysical characterizations have permitted to obtain their relevant properties needed for the design of thermal energy storage systems such as latent heat, melting/solidification temperatures, thermal conductivity and specific heat. Also, the thermal stability study has been accomplished in order to analyze the thermal performance of these materials after 700 cycles. Finally, the chemical compatibility tests between the $Mg_{70}Zn_{24.9}Al_{5.1}$ alloy and the 304, 304L, 316 and 316L stainless steels have been performed. The results have confirmed the high potential of the investigated alloys for thermal energy storage application.

© 2015 The Authors. Published by Elsevier Ltd. This is an open access article under the CC BY-NC-ND license (<http://creativecommons.org/licenses/by-nc-nd/4.0/>).

Peer review by the scientific conference committee of SolarPACES 2014 under responsibility of PSE AG

Keywords: Thermal energy storage, Metal alloys, Mg-Zn-Al system, phase change material, latent heat storage, thermal conductivity.

* Corresponding author. Tel.: +34 945297108.
E-mail address: afaik@cicenergigune.com

1. Introduction

In the last years, the development of thermal energy storage (TES) systems has become an interesting way to upgrade the concentrated solar power (CSP) technologies. TES systems help to extend the power generation during low irradiance periods or at night allowing the decoupling of the solar radiation and electricity production times [1,2].

Current heat storage technologies are mainly based on sensible heat storage in the double molten salt tank concept. However, latent heat storage (LHS) has become one of the most interesting alternatives due to the high storage energy density and the quasi-constant operation temperature associated with the phase transition. Several types of materials (so called phase change materials - PCM) have been studied for latent heat storage [3]. However, the major drawback of these materials is their low thermal conductivity which implies low heat transfer rates. In the last years, a very important research effort is being done in order to solve this limitation [4-6].

An alternative to increase the thermal transport behavior of the TES system is the use of metal and metal alloys as PCMs [7-9]. They usually present high density and thermal conductivity values around two or three order of magnitude higher than the materials currently used for heat storage. A TES system based on these materials can provide a fast thermal response and high operation power which might represent a breakthrough concept regarding current storage technologies. This innovative storage concept could contribute to optimize the thermal management and power generation of current CSP plants in different aspects. For example minimizing the impact of; (i) solar radiation fluctuations, which lead to a neat decrease of the generated electricity, (ii) decreasing the operation cost due to a faster and more efficient start-up of the plant and (iii) decreasing the maintenance cost due to an improved protection against thermal shocks of some plant components.

The aim of this study is to investigate eutectic metal alloys as high thermal conductive PCM's for thermal energy storage. Taking into account the operation temperature range in current CSP plants using oil (from 563 K to 660 K) and molten salts (from 563 K to 838 K) as heat transfer fluid (HTF), eutectic alloys with melting and solidification points in the common temperature range have been chosen. For this purpose, the $Mg_{70}Zn_{24.9}Al_{5.1}$ and $Zn_{85.8}Al_{8.2}Mg_6$ ternary eutectic alloys, with theoretical melting points of 611 K and 618 K, respectively, have been identified. After their synthesis, a complete structural and thermo-physical characterization has been performed in order to determine their suitability as storage materials for this kind of applications. Together with appropriate thermo-physical properties, the thermal stability of the selected PCM is also an essential aspect to ensure the long life-time of the storage system [10]. As a consequence, in this work, short and long-term thermal stability experiments have been performed. In addition, the chemical compatibility between the PCM and the containment materials is also a critical issue in order to guarantee the viability of this storage system [11]. For this reason, the chemical compatibility and corrosion tests between the $Mg_{70}Zn_{24.9}Al_{5.1}$ alloy and common stainless steels used as containment materials have been carried out.

2. Materials and methods

2.1. Material synthesis

$Mg_{70}Zn_{24.9}Al_{5.1}$ and $Zn_{85.8}Mg_{8.2}Al_6$ eutectic alloys were synthesized from Mg, Zn and Al ingots with a purity of 99.94 %, 99.995 % and 99.7 % (mass %), respectively. The stoichiometric proportions of the primary metals in the respective alloys were used to prepare pre-alloys with a weight of 60 g of each one. The pre-alloys, previously placed in alumina crucibles, were hermetically closed inside stainless steel reactors under inert argon atmosphere in order to avoid the oxygen presence during the alloying process. The reactors were placed in an electrical muffle furnace and were maintained at 723 K for 10 hours. During the melting process, in order to guarantee the homogeneity of the alloys, an external mechanical movement was applied each 30 minutes. After cooling down at 10 K/min rate, the alloy samples were turned around and the synthesis process was repeated three times. The homogeneity of the prepared materials was confirmed by inductively coupled plasma (ICP - Ultima 2 Horiba) spectrometry.

2.2. Characterization methods

In order to perform a structural characterization of the obtained alloys X-ray powder diffraction (XRPD) (BrukerD8 Advance Diffractometer), scanning electron microscopy (SEM) (Quanta FEG 250) and energy-dispersive X-ray spectrometry (EDX) techniques were used.

Regarding thermophysical properties, the density (ρ) of the alloys was measured at room temperature by helium pycnometry (AccuPyc-II 1340 from Micrometrics). The coefficient of thermal expansion (CTE) in the solid phase was obtained by dilatometry (DIL 402C, Netsch), where, cylindrical samples of 10 mm of diameter and 10-25 mm of length were cycled two times from 298 to 589 K under argon atmosphere. The transition temperatures, latent heat (ΔH) and specific heat (C_p) were obtained by differential scanning calorimetry (DSC) measurements working under argon atmosphere. For the calorimetric analysis three cycles between 473 and 773 K with heating/cooling rates of 10 K/min were carried out. The C_p was obtained by means of the modulated quasi-isothermal DSC technique using alumina crucibles from room temperature up to 723 K. The thermal diffusivity was determined by Laser Flash Apparatus (LFA) in the temperature range from 323 to 723 K and under argon atmosphere. The thermal conductivity was indirectly calculated from density, specific heat and thermal diffusivity measurements by means of the following equation, $\lambda = \rho \cdot C_p \cdot \alpha$.

The thermal stability test was performed by means of short and long term experiments. In the first one, 100 cycles between 553 and 673 K were performed by DSC with heating/cooling rates of 10 K/min and under argon atmosphere. During the cycling the transition temperatures and enthalpies were measured in order to evaluate any possible evolution of the thermal properties of the alloys. The long-term experiment has been carried out in an electrical muffle furnace with the previous experimental conditions and up to 700 cycles. After each 100 cycles a small piece of the sample was analyzed by DSC in order to check any possible variation on the transition enthalpy and temperature.

The compatibility experiments were performed between the $\text{Mg}_{70}\text{Zn}_{24.9}\text{Al}_{5.1}$ eutectic alloy and different type of containments materials. The tested materials were the common stainless steels (SS) used in the construction of the storage tank unit commercially called 304, 304L, 316 and 316L. The stainless steel samples were vertically placed inside of melted alloy contained in alumina crucibles. The samples (alloy + SS) were hermetically closed inside the reactors under argon atmosphere and were heated at 673 K during 672 hours in an electrical muffle furnace. Finally, the samples were polished and analyzed by SEM and EDX techniques.

3. Results and discussion

3.1. Structural analysis

The X-ray diffractograms of the $\text{Mg}_{70}\text{Zn}_{24.9}\text{Al}_{5.1}$ and $\text{Zn}_{85.8}\text{Al}_{8.2}\text{Mg}_6$ eutectic alloys are shown in Figure 1. In order to determine the phase compositions of each material the refinements of the diffractograms were performed using the FullProf package [12]. The $\text{Mg}_{70}\text{Zn}_{24.9}\text{Al}_{5.1}$ alloy pattern shows the presence of two phases: the first one is isostructural to the trigonal $\text{Mg}_{21}\text{Zn}_{25}$ intermetallic phase [13], and the second one is isostructural to the hexagonal Mg phase [14]. According to the isothermal section of the Mg-Zn-Al phase diagram at room temperature [15], the cubic $\text{Mg}_{32}(\text{Al,Zn})_{49}$ intermetallic phase [16] should be present in equilibrium with the observed $\text{Mg}_{21}\text{Zn}_{25}$ and Mg phases but it was not obtained in our experimental data. However, further investigations are required in order to clarify the effect of the preparation conditions on the stabilization of this phase at room temperature.

The $\text{Zn}_{85.8}\text{Al}_{8.2}\text{Mg}_6$ alloy pattern shows the presence of three phases, the first one is isostructural to the cubic Al phase [17], the second one is isostructural to the hexagonal Zn phase [18] and the last one is isostructural to the cubic $\text{Mg}_2\text{Zn}_{11}$ intermetallic phase [19]. In this case, the identified phases are in agreement with the Mg-Zn-Al phase diagram at room temperature [15].

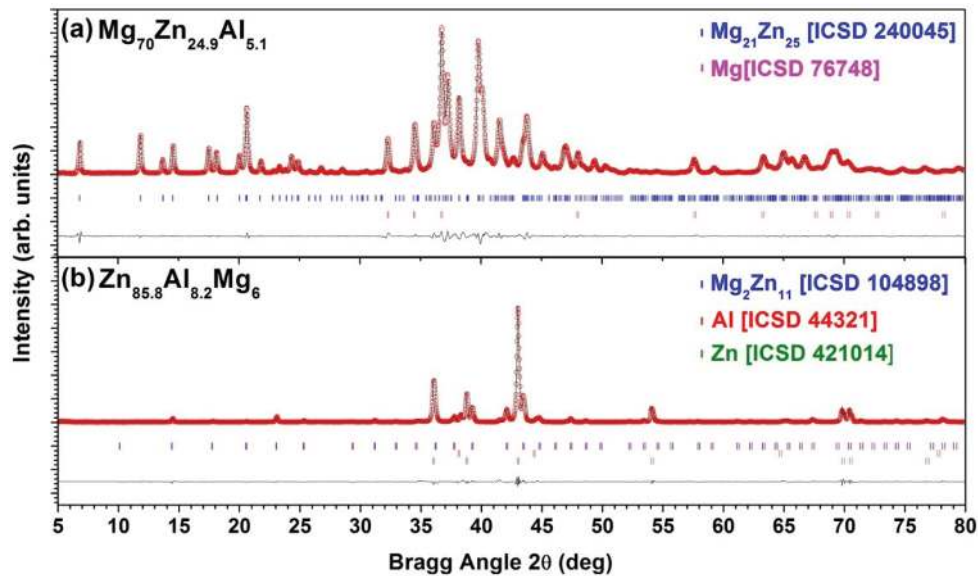


Fig. 1. Experimental (red circles, oo) and calculated (black line, --) X-ray diffraction patterns for the refinements of (a) the $\text{Mg}_{70}\text{Zn}_{24.9}\text{Al}_{5.1}$ and (b) the $\text{Zn}_{85.8}\text{Al}_{8.2}\text{Mg}_6$ alloys. The bars in the lower part of the graphics represent the Bragg peak positions that correspond to the identified phases.

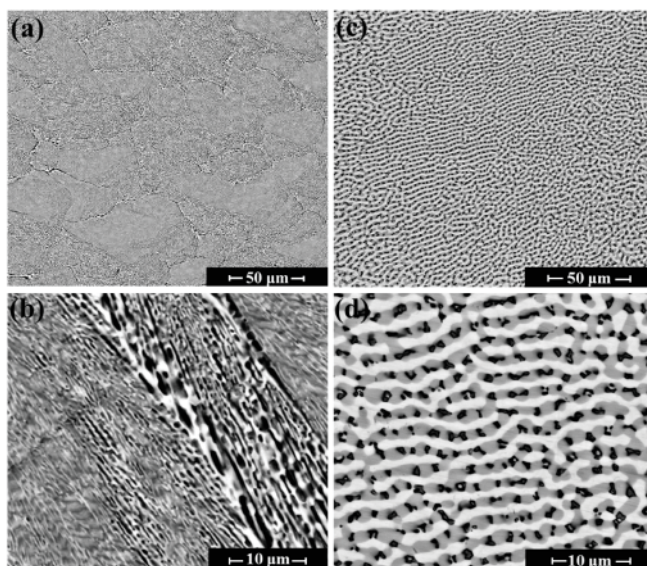


Fig. 2. SEM images of $\text{Mg}_{70}\text{Zn}_{24.9}\text{Al}_{5.1}$ (a,b) and $\text{Zn}_{85.8}\text{Al}_{8.2}\text{Mg}_6$ (c,d) eutectic alloys.

Figure 2 shows the microstructures of the $\text{Mg}_{70}\text{Zn}_{24.9}\text{Al}_{5.1}$ (a) and $\text{Zn}_{85.8}\text{Al}_{8.2}\text{Mg}_6$ (b) eutectic alloys obtained by SEM analysis. The $\text{Mg}_{70}\text{Zn}_{24.9}\text{Al}_{5.1}$ alloy image (a) provided an experimental confirmation of the presence of $\text{Mg}_{21}\text{Zn}_{25}$ and Mg phases. Although an exhaustive microstructural inspection was performed the cubic $\text{Mg}_{32}(\text{Al},\text{Zn})_{49}$ intermetallic phase was not found. The image shows in black colour the isostructural Mg phase and in white colour the isostructural $\text{Mg}_{21}\text{Zn}_{25}$ intermetallic phase with no-faceted /no-faceted (nf /nf) binary eutectic structure. The $\text{Zn}_{85.8}\text{Al}_{8.2}\text{Mg}_6$ alloy image (b) shows nf /nf /nf (Al)-(Zn)- $\text{Mg}_2\text{Zn}_{11}$ ternary eutectic structure: in black colour Al isostructural phase, in white colour Zn isostructural phase and in grey colour $\text{Mg}_2\text{Zn}_{11}$ isostructural

intermetallic phase. The scanning electron microscopy (SEM) analyses confirm the results obtained by XRPD measurements.

3.2. Thermophysical characterization

Table 1 shows a summary of the experimental values of thermophysical properties obtained for $\text{Mg}_{70}\text{Zn}_{24.9}\text{Al}_{5.1}$ and $\text{Zn}_{85.8}\text{Al}_{8.2}\text{Mg}_6$ eutectic alloys. As can be observed both materials present very close melting temperatures: the first one melts at 613 K and the second one at 617 K. Higher differences are observed in their enthalpy values (ΔH_m) and densities, showing that the $\text{Mg}_{70}\text{Zn}_{24.9}\text{Al}_{5.1}$ alloy has the highest latent heat value and the lowest density due to the high magnesium content. The calculated energy density shows that $\text{Zn}_{85.8}\text{Al}_{8.2}\text{Mg}_6$ alloy presents a value ($64.376 \cdot 10^7 \text{ J/m}^3$) than the $\text{Mg}_{70}\text{Zn}_{24.9}\text{Al}_{5.1}$ alloy ($44.274 \cdot 10^7 \text{ J/m}^3$).

Table 1: The experimental values of thermophysical properties obtained for $\text{Mg}_{70}\text{Zn}_{24.9}\text{Al}_{5.1}$ and $\text{Zn}_{85.8}\text{Mg}_{8.2}\text{Al}_6$ eutectic alloys.

	T_m	ΔH_m	ρ	CTE _{average}	C_p		α			λ		
	(K)	(10^3 J/kg)	(kg/m^3)	(10^{-6} K^{-1})	(J/kg·K)	(J/kg·K)	(10 ⁻⁶ m ² /s)			(W/m·K)		
$T(\text{K})$			298	373-523	298	573	323	573	673	323	573	673
$\text{Mg}_{70}\text{Zn}_{24.9}\text{Al}_{5.1}$	613	157	2820	24	690	830	23	26	16	47	59	38
$\text{Zn}_{85.8}\text{Al}_{8.2}\text{Mg}_6$	617	104	6190	34	410	530	25	21	9	59	55	31

The linear coefficients of thermal expansion (CTE) in solid phase showed values approximately constant for both alloys in all measured interval. The $\text{Zn}_{85.8}\text{Al}_{8.2}\text{Mg}_6$ eutectic alloy shows a higher linear coefficient value due to its high Zn content. The obtained values are in concordance with the linear thermal expansion coefficients of the pure metals: $39.7 \cdot 10^{-6}$, $23.6 \cdot 10^{-6}$ and $25.2 \cdot 10^{-6} \text{ K}^{-1}$ for Zn, Al and Mg, respectively. Both alloys present CTE slight higher than those of the commonly used stainless steels in the storage unit construction (around $17 \cdot 10^{-6} \text{ K}^{-1}$).

The obtained specific heats (C_p) for both eutectic alloys are noticeably different. Taking into account the C_p values of the Zn, Al and Mg pure metals (390, 900 and 1020 J/kg·K at RT, respectively) the $\text{Mg}_{70}\text{Zn}_{24.9}\text{Al}_{5.1}$ alloy presents the highest value due to its higher Mg content and the $\text{Zn}_{85.8}\text{Al}_{8.2}\text{Mg}_6$ alloy the lowest value due to its higher Zn content. The obtained results are in a good agreement with the obtained from the calculation performed in [9]. This model gives values close to the experimental ones, showing around 720 and 810 J/kg·K for the $\text{Mg}_{70}\text{Zn}_{24.9}\text{Al}_{5.1}$ and around 430 and 480 J/kg·K for $\text{Zn}_{85.8}\text{Al}_{8.2}\text{Mg}_6$ alloys at 298 and 573 K, respectively.

The thermal diffusivity (α) and the thermal conductivity (λ) are the most important parameters in the metallic material heat transport properties definition which are related by the equation $\alpha = \lambda / \rho \cdot C_p$. Table 1 shows the experimental values of thermal diffusivities and the calculated thermal conductivities at 323 K, 573 K (in solid phase) and 673 K (in the liquid phase). - The obtained values for both properties are almost constant in the solid phase and decrease around to the half value in the liquid phase. In any case, the obtained values in solid and liquid phases are still very high around two orders of magnitude higher than those of the inorganic PCMs.

3.3. Long-term thermal stability (cyclability)

Figures 3 (a) and (b) show the results of the short-term thermal stability experiments (100 cycles) performed by DSC technique for both eutectic alloys. Each 10 cycles the corresponding curves are plotted to demonstrate the repeatability of the results. Although small changes on the peak shapes are found the melting temperature and enthalpy remain constant. Finally, Figure 3 (c) shows the results of the long-term thermal stability experiment (700 cycles) performed by means of an electrical furnace for the $\text{Mg}_{70}\text{Zn}_{24.9}\text{Al}_{5.1}$ alloy. The heating latent heat and melting temperatures at before and after 50, 100, 200, 300, 500 and 700 cycles are indicated with lines with circles and triangles, respectively. As it is shown in the graph (c), both values are constants up to 700 cycles. Thus, cycling

stability in term of melting and solidification has been demonstrated for at least 700 cycles in the case of $\text{Mg}_{70}\text{Zn}_{24.9}\text{Al}_{5.1}$ alloy and at least 100 cycles in the case of $\text{Zn}_{85.8}\text{Al}_{8.2}\text{Mg}_6$ alloy.

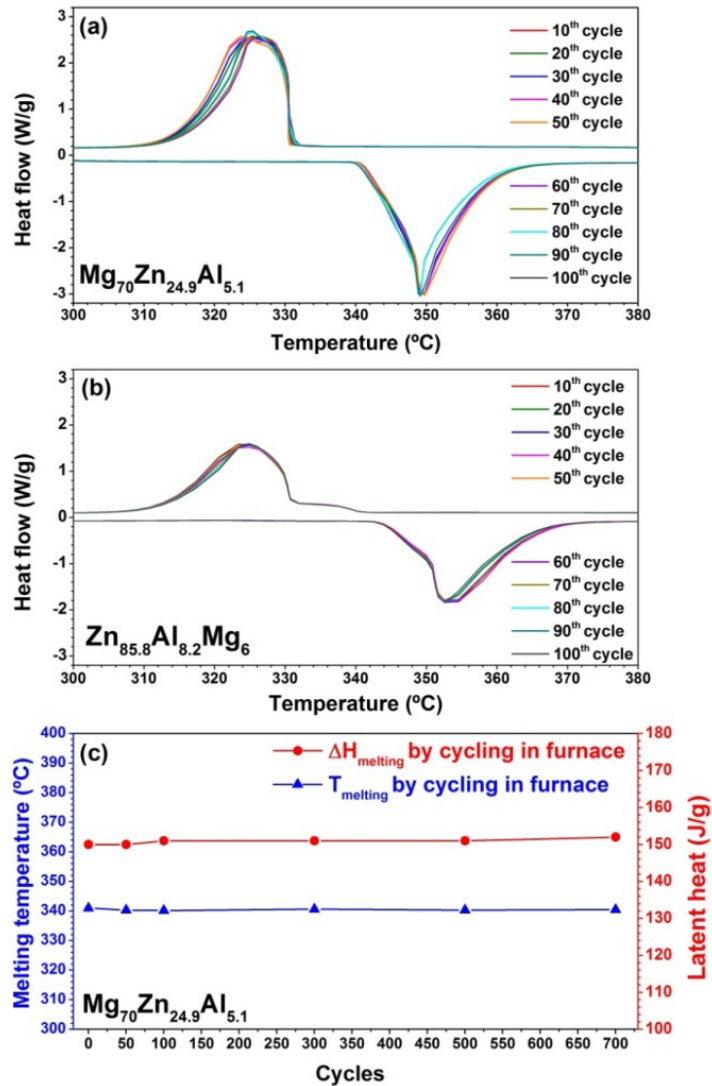


Fig. 3. Short and long-term thermal stability experiment results for the $\text{Mg}_{70}\text{Zn}_{24.9}\text{Al}_{5.1}$ and $\text{Zn}_{85.8}\text{Al}_{8.2}\text{Mg}_6$ eutectic alloys. Several DSC curves after every 10 cycles of the short-term thermal stability experiment for the $\text{Mg}_{70}\text{Zn}_{24.9}\text{Al}_{5.1}$ eutectic alloy (a), and for the $\text{Zn}_{85.8}\text{Al}_{8.2}\text{Mg}_6$ eutectic alloy (b) and (c) the heating latent heat (circles) and the melting temperatures (triangles) before and after 50, 100, 200, 300, 500 and 700 cycles of the long-term thermal stability experiment for the $\text{Mg}_{70}\text{Zn}_{24.9}\text{Al}_{5.1}$ eutectic alloy.

3.4. Compatibility between the eutectic alloys and containments materials

The results of the compatibility analysis performed between the SS304L containment material and the $\text{Mg}_{70}\text{Zn}_{24.9}\text{Al}_{5.1}$ eutectic alloy are shown in Figure 4. The SEM image shows a clear division between both surfaces of the materials, where the $\text{Mg}_{70}\text{Zn}_{24.9}\text{Al}_{5.1}$ surface is on the left and the 304L stainless steel surface is on the right. In the corresponding EDX maps the most representative elements of each material have been selected: the Mg and Zn from the $\text{Mg}_{70}\text{Zn}_{24.9}\text{Al}_{5.1}$ alloy and Cr and Fe from 304L stainless steel. By the displayed EDX maps, no migration of the Mg and Zn elements in right direction and no migration of the Fe and Cr elements in left direction

are observed. The same results are obtained with the other selected stainless steels and no chemical corrosion has happened and demonstrates that the investigated metal alloy is fully compatible with the four common stainless steels (SS304, SS304L, SS316 and SS316L).

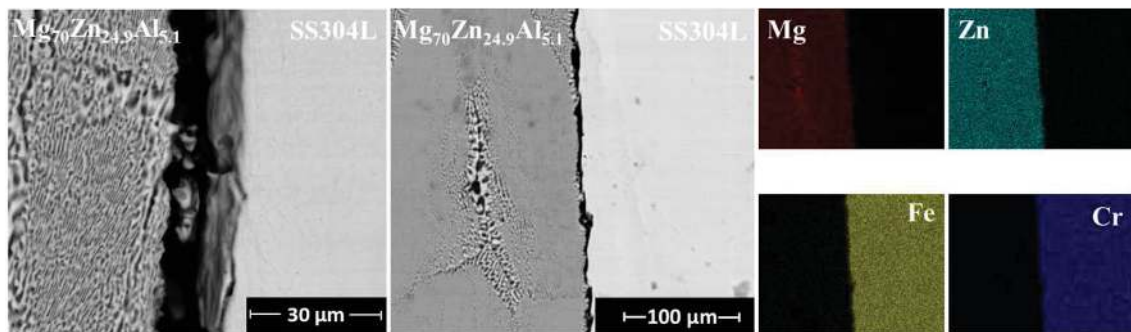


Fig. 4. The SEM images and corresponding EDX maps of the compatibility experiments between the Mg₇₀Zn_{24.9}Al_{5.1} eutectic alloy and the 304L stainless steel containment material.

4. Conclusions

In general, this investigation has shown the high potential of Mg-Zn-Al ternary system in the thermal energy storage frame. The structural characterization and thermophysical determination of the selected ternary eutectic alloys confirm that both compositions are suitable to be used as high thermal conductive phase change materials. Among measured thermal properties, the remarkable high density of the Zn_{85.8}Al_{8.2}Mg₆ eutectic alloy leads to higher energy storage capacity, in addition to the high thermal conductivities of both alloys, can provide a new concept of high power TES system.

The performed thermal stability experiments have shown promising results in order to ensure the long-term thermal performance of PCM in TES system, where, a good thermal stability was observed for at least 100 cycles for the Zn_{85.8}Al_{8.2}Mg₆ eutectic alloy and for at least 700 cycles for the Mg₇₀Zn_{24.9}Al_{5.1} eutectic alloy.

Finally, the corrosion tests demonstrate the full chemical compatibility of the Mg₇₀Zn_{24.9}Al_{5.1} eutectic alloy with some of the most common stainless steels used in the construction of the TES tanks.

Acknowledgements

The authors would like to thank the Department of Industry, Innovation, Commerce and Tourism of the Basque Government for funding the ETORTEK CIC Energigune-2011 research program. The authors would also like to thank Naira Soguero for her technical support.

References

- [1] Gil A, Medrano M, Martorell I, Lázaro A, Dolado P, Zalba B, Cabeza LF. State of the art on high temperature thermal energy storage for power generation. Part1-Concepts, materials and modellization, *Renew Sust Energy Rev*, (2010) Vol.14-1: 31-5.
- [2] Medrano M, Gil A, Martorell I, Potau X, Cabeza LF. State of the art on high temperature thermal energy storage for power generation. Part2-Case studies. *Renew Sust Energy Rev*, (2010) Vol.14-1: 56-72.
- [3] Laing D, Bauer T, Lehmann D, Bahl C. Development of a thermal energy storage system for parabolic trough power plants with direct steam. *J. Sol. Energy Eng.*, (2010) 132(2): 021011.1–021011.8.
- [4] Liu M, Saman W, Bruno F. Review on storage materials and thermal performance enhancement techniques for high temperature phase change thermal storage systems., *Renew Sust Energy Rev*, (2012) 16(4): 2118–2132.
- [5] Cárdenas B, León N. High temperature latent heat Thermal energy storage: phase change materials, design considerations and performance enhancement techniques. *Renew Sust Energy Rev*, (2013) 27: 724–737.

- [6] Jegadheeswaran S, Pohekar SD. Performance enhancement in latent heat thermal storage system: a review. *Renew Sust Energy Rev*, (2009) 13: 2225–2244.
- [7] Birchenall CE, Reichman AF. Heat storage in eutectic alloys. *Metall Trans A* (1980) 11(8): 1415–1420.
- [8] Farkas D, Birchenall CE. New eutectic alloys and their heats of transformation. *Metall Trans A*, 16A(1985) 323–328.
- [9] Rodríguez-Aseguinolaza J, Blanco-Rodríguez P, Risueño E, Tello MJ, Doppiu S. Thermodynamic study of the eutectic Mg₄₉–Zn₅₁ alloy used for thermal energy storage. *J Therm Anal Calorim*, (2014) 117:93–99.
- [10] Rathod MK, Banerjee J. Thermal stability of phase change materials used in latent heat energy storage systems: A review. *Renew Sust Energy Rev* (2013) 18: 246–258.
- [11] Sun JQ, Zhang RY, Liu ZP, Lu GH. Thermal reliability test of Al-34%Mg-6%Zn alloy as latent heat storage material and corrosion of metal with respect to thermal cycling”, *Energy Convers. Manage.*, (2007) 48(2): 619–624.
- [12] Rodriguez-Carvajal J, Roisnel T. FullProf.98 and WinPLOTR New Windows 99/NT Applications for Diffraction. Commission for Powder Diffraction, International Union for Crystallography, 20 (1998) 35-36.
- [13] Cěrný R, Renaudin G. The intermetallic compound Mg₂₁Zn₂₅. *Acta Crystallogr., Sect. C58* (2002) i154-i155.
- [14] Straumanis ME. The precision determination of lattice constants by the powder and rotating crystal methods and applications. *Appl. Phys* 20 (1949) 726-734.
- [15] Liang H, Chen SL, Chang YA. A thermodynamic description of the Al-Mg-Zn system. *Metall. Mater. Trans.* 28A (1997) 1725-1734.
- [16] Bergman G, Waugh JLT, Pauling L. The crystal structure of the metallic phase Mg₃₂ (Al, Zn)₄₉. *Acta Crystallogr.*, 10 (1957) 254-259.
- [17] Cooper AS. Precise lattice constants of germanium, aluminum, gallium arsenide, uranium, sulphur, quartz and sapphire. *Acta Cryst.*(1962) 15(6): 578-82.
- [18] Martinez O et al. Grows of Zn O nanowires through thermal oxidation of metallic zinc films on Cd Te substrates. *J. Alloys Compd.* (2011) 509(17): 5400-07.
- [19] Samson S. Die Kristallstruktur des Mg₂ Zn₁₁. Isomorphie zwischen Mg₂ Zn₁₁ und Mg₂ Cu₆ Al₅. *Acta Chem. Scand.* (1949) 3:835-43.